

500 MeV PROTON BEAM LINE FOR KEK BOOSTER
SYNCHROTRON UTILIZATION FACILITY

I. Sakai, H. Someya, T. Adachi, Y. Irie and H. Sasaki

National Laboratory for High Energy Physics

Magnet System

The layout of the 500 MeV proton beam line is shown in Fig.1. The total length of the beam line is about 80 m. The magnet system is composed of 23 quadrupole magnets, 2 horizontal bending magnets, 1 pulse magnet for beam switching, and 6 steering magnets.

Quadrupole Magnet

The dimensions of the quadrupole magnet are as follows. The bore radius is 57 mm, and geometrical length is 300 mm. The pole face is hyperbolic, and end cut correction was made for uniformity of effective length of the field gradient.¹⁾ About all of 23 quadrupole magnets, transverse distribution of the field gradient and the effective length of the field gradient were measured carefully by the method of displacing twin search coils.²⁾ The accuracy of the measurements were better than 1×10^{-4} of the field gradient on the median plain. The example of the measured value is shown in Figs. 2 and 3. The integrated values of nonlinear field over the useful aperture, ± 75 mm on the median plain, were less than 0.1 % of the field gradient on the median plain. The measured value of each magnet is expanded in Taylor series as,

$$\frac{\partial^2 B_z(x)}{\partial x^2} / \frac{\partial B_z(0)}{\partial x} = b_2 + b_3 x + \frac{b_4}{2!} x^2 + \frac{b_5}{3!} x^3 + \frac{b_6}{4!} x^4 + \frac{b_7}{5!} x^5$$
$$L_G(x)/L_G(0) = L_0 + L_1 x + \frac{L_2}{2!} x^2 + \frac{L_3}{3!} x^3 + \frac{L_4}{4!} x^4 + \frac{L_5}{5!} x^5$$

Coefficients correspond to multipole components. The distribution of each multipole component of 23 quadrupole magnet is shown in Fig.4. The effect of the fabrication error to the nonlinear field is estimated³⁾, and the value was confirmed experimentally by making intentional deviation of the pole. The sextupole component b_2 is induced by asymmetrical error of the magnet. As in Fig.4, the average value of the b_2 is 8×10^{-5} (cm^{-1}), and the standard deviation is 1.6×10^{-4} (cm^{-1}). The corresponding estimated value of asymmetrical deviation of the pole face is about 30 μm with average value and about 58 μm with standard deviation. The octupole component b_3 is induced by symmetrical error of the magnet. As in Fig.4, the average value of the b_3 is -1.6×10^{-5} (cm^{-2}) and the standard deviation is 6×10^{-5} (cm^{-2}). The corresponding estimated value of symmetrical deviation of the pole face is about 9 μm with average value, and 34 μm with standard deviation. Absolute value of the effective length was obtained by the point-to-point measurement of the field gradient along the magnet axis. It is 341 mm long, and the radial distribution is less than 1 mm over the useful aperture.

Vacuum

The vacuum chambers of the beam line were mainly composed of aluminum alloys for the purpose of reducing residual radioactivity. Metal gaskets were used at all of the flange connection. A quantity of leakage from each flange connection and welding portion are less than 1×10^{-10} Torr ls^{-1} for helium. The beam line is evacuated by a ion pump of 1000 ls^{-1} , the maximum pressure less than 10^{-6} Torr was easily performed.

Beam Transport

Proton beam had been transported to Utilization Facility successfully. The beam profiles are observed by secondary emission type profile monitors and the beam intensity monitors. The observed profile is shown in Fig.5. The abscissa is graduated in cm. The monitoring positions are indicated in Fig.1, good agreement between observed and designed values was obtained. The lost beam through the beam line is negligible small.

Reference

- 1) M. Kumada et al; Proceeding of the 2 nd symposium on accelerator science and technology (1978) p.73.
- 2) M. Kumada et al; Proceeding of the 2 nd symposium on accelerator science and technology (1978) p.75.
- 3) Robert J. Lari et al; Calculation of the harmonic content of asymmetrical quadrupole magnets January 24, 1967, RJL/GJB-2, Argonne.

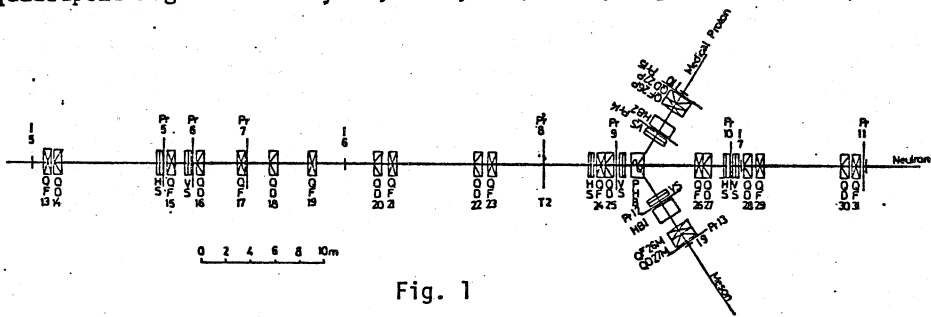


Fig. 1

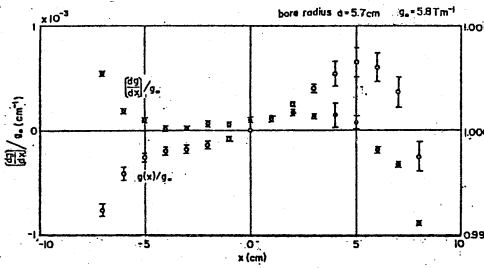


Fig. 2

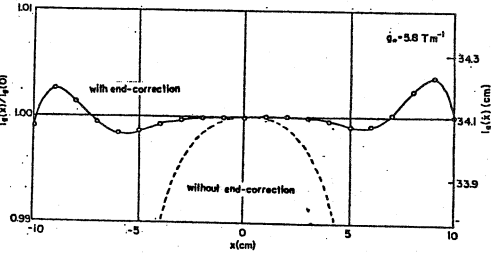


Fig. 3

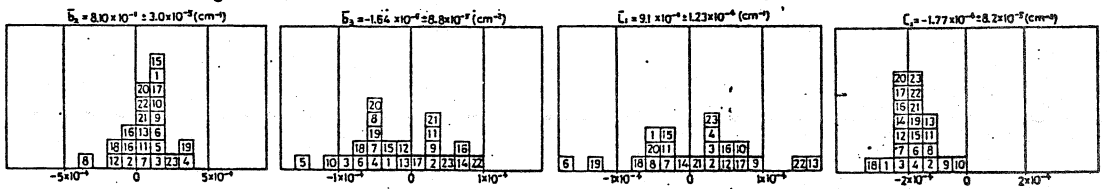


Fig. 4

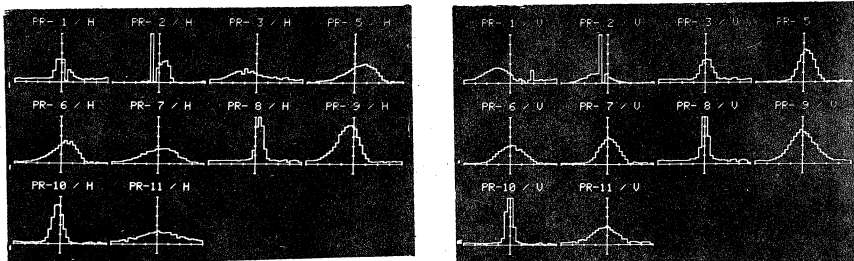


Fig. 5